Stepwise Construction of Extra-Large Heterometallic Calixarene-Based Cages

ARTICLE *in* INORGANIC CHEMISTRY · MARCH 2015

Impact Factor: 4.76 · DOI: 10.1021/ic502677g

Inorganic Chemistry

Article

pubs.acs.org/IC

Stepwise Construction of Extra-Large Heterometallic Calixarene-Based Cages

Kongzhao Su,[†,‡] Feilong Jiang,[†] Jinjie Qian,[†,‡] Lian Chen,[†,‡] Jiandong Pang,[†,‡] Salem M. Bawaked,[§] Mohamed Mokhtar,[§] Shaeel A. Al-Thabaiti,[§] and Maochun Hong*[,†]

[†]State Key Laboratory of Structural Chemistry, Fujian Institute of Research on the Structure of Matter, Chinese Academy of Sciences, Fuzhou, 350002, China

[§]Department of Chemistry, Faculty of Science, King Abdulaziz University, Jeddah, 21589, Saudi Arabia

[‡]University of the Chinese Academy of Sciences, Beijing, 100049, China

Supporting Information

ABSTRACT: Utilizing presynthesized large $Na_2Ni_{12}Ln_2$ clusters (Ln = Dy and Tb) supported by calixarene as molecular building blocks (MBBs), we have obtained a series of cationic trigonal prismatic heterometallic organic nanocages (HMONCs) with tunable sizes through a stepwise method. Specially, in each structure of the HMONCs, three linear dicarboxylate linkers substitute the peripheral coordinated acetate ligands of two $Na_2Ni_{12}Ln_2$ clusters to form an unprecedented $Na_4Ni_{24}Ln_4$ HMONC through a M_2L_3 condensation. Moreover, magnetic study reveals that the $Na_2Ni_{12}Dy_2$ core retains its slow magnetic relaxation behavior. Gas sorption behaviors of these HMONCs were also studied. To the best of our knowledge, these HMONCs built from large heterotrimetallic $Na_2Ni_{12}Ln_2$ MBBs, which are based on smaller Ni_4-calix ones, have not been reported in any other cages to date. In addition, this research also provides a new strategy for the design and construction of HMONCs with predictable structures and functional properties.

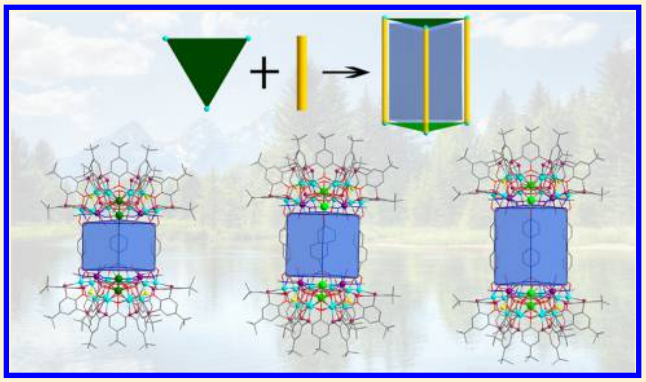

INTRODUCTION

Metal−organic nanocages (MONCs) with well-defined hollow structures have received much attention in recent years, not only because of their fascinating structural beauty[1] but also due to their promising applications in gas separation and storage,[2] host−guest recognition,[3] drug delivery and release,[4] enzyme-mimicking supramolecular catalysis,[5] and so on.[6] A variety of MONCs based on one metal ion or paddle-wheel subunits as the nodes have been well developed.[2,7] However, discrete MONCs constructed by polymetallic molecular building blocks (MBBs) have been rarely reported.[8] Moreover, those polymetallic MBBs are usually *in situ* generated by accident or by an empirical method. In fact, it is very scarce to construct cages using presynthesized polymetallic clusters as the vertexes.[9]

Calixarenes, the macrocyclic host molecules composed of phenolic units and methylene/heteroatom bridges, have been extensively used to construct various fascinating polymetallic compounds.[10] In the past few years, our group and others have prepared several intriguing coordination cages based on the shuttlecock-like TM_4-calix (TM = transition metals) MBBs. Generally speaking, these MBBs are *in situ* generated and they hold the desired curvature and can be further bridged by different ligands into octahedral M_{24} (M = Fe, Co and Ni), tetragonal-prismatic Co_{32} MONCs, and so forth in a one-pot reaction.[11] Interestingly, these MONCs are different from other cages, because they possess both inner voids and well-known calixarene cavities, which make them potential materials in selective and void-directed adsorption/recognition.[11b] Despite the fact that calixarenes are facile to construct MONCs, the discrete cages with heterometallic calixarene-based entities as building blocks have not been reported, which contain multiple metal sites and may endow new physicochemical properties.[12]

Very recently, our group reported two large vertex-fused tricubane $Na_2Ni^{II}_{12}Ln^{III}_2$ (Ln = Dy for **1a**, and Tb for **1b**) clusters supported by *p-tert*-butylthiacalix[4]arene (H_4BTC4A, Scheme 1, in the Supporting Information) under solvethermal conditions, of which compound **1a** exhibits slow magnetic relaxation behavior of single molecule magnet nature.[13] X-ray structural analyses reveal that both clusters possess three Ni_4-BTC4A MBBs in an up-to-up fashion linked by two sodium cations, two lanthanide cations, and other anions including two chlorine, four hydroxide, and six acetate anions (Figure 1). Most importantly, it is found that compounds **1a** and **1b** are easily dissolved in *N*,*N*′-dimethylformamide (DMF) solvent

Received: November 6, 2014

DOI: 10.1021/ic502677g
Inorg. Chem. XXXX, XXX, XXX−XXX

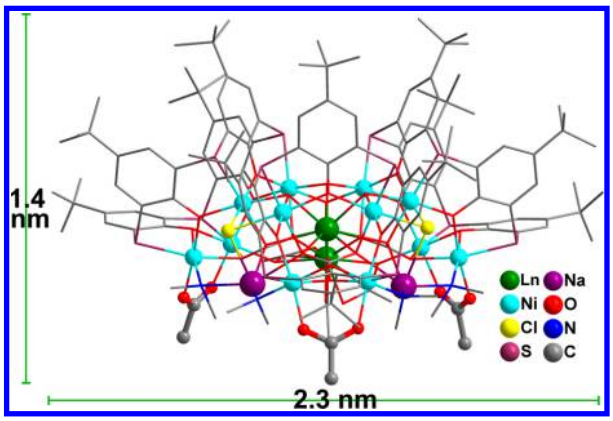

Figure 1. Molecular structure of $Na_2Ni^{II}_{12}Ln^{III}_2$ cluster. The bold bonds highlight the peripheral bridging acetate anions; hydrogen atoms are omitted for clarity.

and still remain intact, which is confirmed by mass spectrometry (MS) (Figure S4 and S5, in the Supporting Information). Thus, we reason that the large $Na_2Ni_{12}Ln_2$ clusters could serve as useful MBBs and therefore possibly be useful for constructing heterometallic organic nanocages (HMONCs), if three peripheral acetates are substituted by bridging ligands such as linear dicarboxylates through a stepwise method (Figure 2). Herein, we present five extra-large heterometallic calixarene-based coordination nanocages, $[Na_4Ni_{24}Ln_4(BTC4A)_6L_3(CO_3)_6(OH)_8Cl_4(H_2O)_{10}]^{10+}$ (HMONC-**1**, Ln = Dy, L = BDC; HMONC-**2**, Ln = Dy, L = NDC; HMONC-**3**, Ln = Dy, L = BPDC; HMONC-**4**, Ln = Dy, L = BIPY; HMONC-**5**, Ln = Tb, L = BDC), which are synthesized by the above-mentioned method. To the best of our knowledge, these HMONCs present the first examples of nanoscale cages constructed by high-nuclearity heterotrimetallic MBBs.

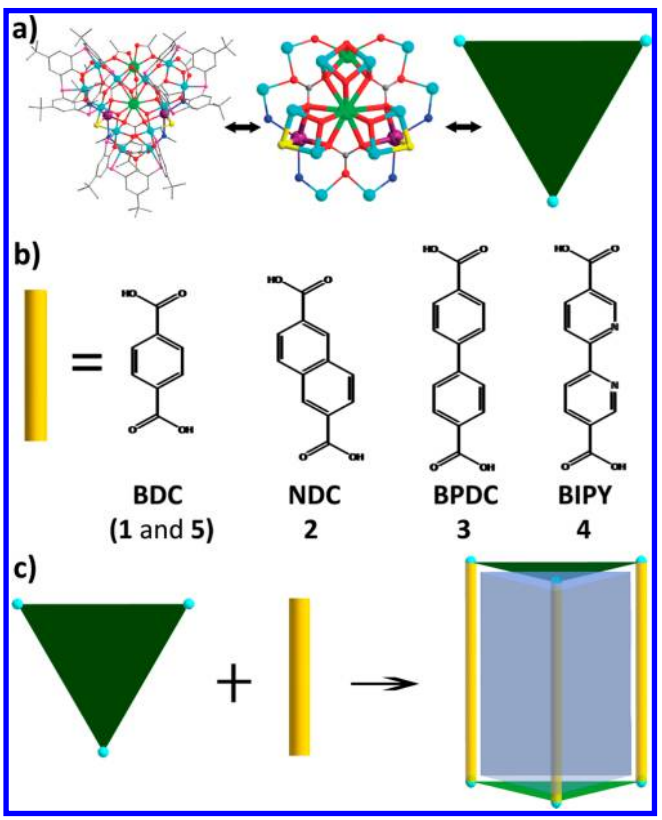

Figure 2. (a) Molecular structure of $Na_2Ni_{12}Ln_2$ cluster (left); vertex-fused tricubane core (middle); the green triangle stands for the MBB (right). Color code as in Figure 1. (b) Linear dicarboxylic acid linkers. (c) Schematic representation of the formation of the HMONCs.

EXPERIMENTAL SECTION

Physical Measurement. Elemental analyses were performed on a German Elementary Varil EL III instrument. Powder X-ray diffraction (PXRD) was recorded by a RIGAKU-DMAX2500 X-ray diffractometer using Cu Kα radiation (λ = 0.154 nm). Mass spectra were collected using a DECAX-30000 LCQ Deca XP mass spectrometer with electrospray ionization (ESI). Thermogravimetric analyses (TGA) were carried out on preweighted samples in a nitrogen stream using a NETZSCH STA 449C instrument. Magnetic susceptibilities were carried out on a Quantum Design PPMS-9T and MPMS-XL systems. Single gas adsorption measurements were performed in the Accelerated Surface Area and Porosimetry 2020 (ASAP 2020) System. All samples were activated for gas sorption studies by exchanging with methanol solution for 3 days and then heating at 100 °C for 8 h under vacuum.

Synthesis Procedures. *p-tert*-Butylthiacalix[4]arene (formula: $C_{40}H_{48}O_4S_4$)[18] and $Na_2Ni^{II}_{12}Ln^{III}_2$ (Ln = Dy for **1a**, and Tb for **1b**) clusters[13] were prepared as reported in the literature. 1,4-Benzenedicarboxylic acid, 2,6-naphthalenedicarboxylic acid, 4,4′-biphenyldicarboxylic acid, and 2,2′-bipyridine-5,5′-dicarboxylic acid were commercially available and used as received. Other solvents were of reagent grade quality obtained from commercial sources and used without further purification.

Syntheses of $[Na_2Ni^{II}_{12}Ln^{III}_2(BTC4A)_3(CO_3)_3(OH)_4(Cl)_2(OAc)_6(dma)_4]$·2OAc·0.5dma·3MeCN·8DMA (Ln = Dy for 1a, and Tb for 1b). In a general procedure, a mixture of H_4BTC4A (0.1 mmol, 72 mg), $NiCl_2·6H_2O$ (0.4 mmol, 95 mg), $Ln(OAc)_3·6H_2O$ (0.3 mmol, 132 mg), and Na_2CO_3 (0.2 mmol, 21 mg) in DMA/CH_3CN/Et_3N (6/3/0.5 mL) was sealed in a 25 mL Teflon-lined autoclave at 130 °C for 6 days and then cooled slowly for 1 day to room temperature. Green blocky crystals of **1a,b** were obtained by slow concentration of the filtrate at room temperature for several days.

Synthesis of HMONC-1. A mixture of compound **1a** (~100 mg) and H_2BDC (0.2 mmol, 33 mg) in 5 mL of DMF with an additional five drops of water was sealed in a 23 mL glass vial, which was heated at 85 °C for 1 day, and cooled down to room temperature. After washing by fresh DMF, the green hexagonal shaped crystals were obtained in *ca.* ~80% yield based on compound **1a**. Elemental analysis: Anal. Calcd for $[Na_4Ni_{24}Dy_4(BTC4A)_6(BDC)_3(CO_3)_6(OH)_8(Cl)_4(H_2O)_{10}(dma)_8]$·10OAc: C, 42.18; H, 4.51; N, 1.29. Found (after being exchanged by methanol and dried in vacuum): C, 42.02; H, 4.36; N, 1.32.

Synthesis of HMONC-2. A mixture of **1a** (~100 mg) and H_2NDC (0.15 mmol, 32 mg) in DMF (2.5 mL) and 1-methyl-2-pyrrolidinone (NMP) (2.5 mL) with an additional five drops of water was sealed in a 23 mL glass vial, which was heated at 85 °C for 3 days, and cooled down to room temperature. After washing by fresh DMF-NMP (v:v 1:1), the green hexagonal shaped crystals were obtained in *ca.* ~75% yield based on compound **1a**. Elemental analysis: Anal. Calcd for $[Na_2Ni_{24}Dy_4(BTC4A)_6(NDC)_3(CO_3)_6(OH)_8(Cl)_4(H_2O)_{10}(dma)_8]$·10OAc: C, 43.09; H, 4.50; N, 1.26. Found (after being exchanged by methanol and dried in vacuum): C, 42.96; H, 4.62; N, 1.29.

Synthesis of HMONC-3. Synthesis was as for HMONC-**2**, except H_2BPDC (0.15 mmol, 36 mg) was used in place of H_2NDC. Yield: ~68% based on compound **1a**. Elemental analysis: Anal. Calcd for $[Na_2Ni_{24}Dy_4(BTC4A)_6(BPDC)_3(CO_3)_6(OH)_8(Cl)_4(H_2O)_{10}(dma)_8]$·10OAc: C, 43.72; H, 4.49; N, 1.34. Found (after being exchanged by methanol and dried in vacuum): C, 42.68; H, 4.39; N, 1.28.

Synthesis of HMONC-4. Synthesis was as for HMONC-**2**, except H_2BIPY (0.15 mmol, 36 mg) was used in place of H_2NDC. Yield: ~55% based on compound **1a**. Elemental analysis: Anal. Calcd for $[Na_2Ni_{24}Dy_4(BTC4A)_6(BIPY)_3(CO_3)_6(OH)_8(Cl)_4(H_2O)_{10}(dma)_8]$·

DOI: 10.1021/ic502677g
Inorg. Chem. XXXX, XXX, XXX−XXX

Table 1. Crystal Data and Structure Refinement Parameters for Title HMNOCs

	HMONC-1	HMONC-2	HMONC-3	HMONC-4	HMONC-5
formula	$C_{286}H_{360}N_8O_{72}Cl_4S_{24}Na_4Ni_{24}Dy_4$	$C_{298}H_{366}N_8O_{72}Cl_4S_{24}Na_4Ni_{24}Dy_4$	$C_{304}H_{372}N_8O_{72}Cl_4S_{24}Na_4Ni_{24}Dy_4$	$C_{298}H_{366}N_{14}O_{72}Cl_4S_{24}Na_4Ni_{24}Dy_4$	$C_{286}H_{360}N_8O_{72}Cl_4S_{24}Na_4Ni_{24}Tb_4$
formula wt	8123.89	8228.09	8352.19	8358.11	8109.59
cryst syst	hexagonal	hexagonal	hexagonal	hexagonal	hexagonal
space group	*P*63/*m*	*P*63/*m*	*P*63/*m*	*P*63/*m*	*P*63/*m*
a (Å)	23.3919(6)	23.5399(2)	23.41720(10)	23.3568(2)	23.3815(2)
b (Å)	23.3919(6)	23.5399(2)	23.41720(10)	23.3568(2)	23.3815(2)
c (Å)	61.3970(19)	65.7940(4)	70.1696(3)	69.7927(6)	61.3635(7)
α (deg)	90	90	90	90	90
β (deg)	90	90	90	90	90
γ (deg)	120	120	120	120	120
V (Å^3)	29094.3(14)	31573.7(4)	33323.4(2)	32973.7(5)	29052.6(5)
T/K	100(2)	100(2)	100(2)	100(2)	100(2)
Z	2	2	2	2	2
R_{int}	0.1257	0.1146	0.0933	0.1068	0.0990
data collected	100028	69230	104746	114801	94126
unique data	18407	19971	22240	20175	19492
GOF on F^2	0.968	1.093	1.094	1.029	1.080
R1[a] [$I > 2\sigma(I)$]	0.0866	0.0880	0.0766	0.0881	0.0825
wR2[b]	0.2288	0.2445	0.2157	0.2328	0.2304

[a] $R1 = \sum||F_o| - |F_c||/\sum|F_o|$. [b] $wR2 = \{\sum[w(F_o^2 - F_c^2)^2]/\sum[w(F_o^2)^2]\}^{1/2}$.

10OAc: C, 42.82; H, 4.47; N, 2.20. Found (after being exchanged by methanol and dried in vacuum): C, 43.12; H, 4.50; N, 2.26.

Syntheses of HMONC-5. Synthesis was as for HMONC-**1**, except compound **1b** (~100 mg) was used in place of **1a**. Yield: ~72% based on **1b**. Elemental analysis: Anal. Calcd for $[Na_2Ni_{24}Tb_4(BTC4A)_6(BDC)_3(CO_3)_6(OH)_8(Cl)_4(H_2O)_{10}(dma)_8]\cdot 10OAc$: C, 42.25; H, 4.52; N, 1.29. Found (after being exchanged by methanol and dried in vacuum): C, 42.48; H, 4.34; N, 1.24.

X-ray Data Collection and Structure Determination. The intensity data for all five HMONCs was collected with a copper microfocus X-ray source (λ = 1.5406 Å) on a SuperNova Dual wavelength diffractometer with an Atlas CCD detector at 100(2) K. The crystal structures were solved by direct methods, the metal atoms were located from the E-maps, and other non-hydrogen atoms were derived from the successive difference Fourier peaks. The structures were refined by using full-matrix least-squares on F^2 by the *SHELXTL-97* program package.[19] The diffraction data were treated by the "SQUEEZE" method as implemented in PLATON to remove diffuse electron density associated with those badly disordered solvent molecules and counter acetate anions.[20] This had the effect of dramatically improving the agreement indices. All the non-hydrogen atoms were refined anisotropically except some badly disordered atoms and some solvent molecules. Hydrogen atoms of the organic ligands were generated theoretically onto the specific atoms and refined isotropically with fixed thermal factors. Somme hydrogen atoms on coordinated water and dma molecules cannot be generated, but they were included in the molecular formula directly. The unidentified solvent molecules and 10 acetate anions were not included for all the five structures. Disorder was observed in the peripheral Ln, Na, N, and O atoms, with the occupancy factor of 1/3:2/3 for Ln and Na, and with the occupancy factor of 1/3:2/3 for N and O, respectively (Figure S2, in the Supporting Information). These disorders are due to these $Na_4Ni_{24}Ln_4$ HMONCs crystallized in hexagonal system in solid state (with C_6 symmetry). In addition, disorder was also observed in eight carbon atoms in NDC^{2-} ligands with the same occupancy factor of 0.5 in **3**, and two donor nitrogen and two carbon atoms (N3, C46, and their symmetry equivalents) in $BIPY^{2-}$ ligands with the occupancy factor of 0.5:0.5 for N and C in **4**, respectively. The high R1 and wR2 factors of all HMONCs, which are typical in such a system, might be due to the weak crystal diffractions owing to the structure disorder. Details of the crystallographic data and structure refinement data for the HMONCs are summarized in Table 1. CCDC-1022524−1022528 contain the supplementary crystallographic data for this paper. These data can be obtained free of charge through www.ccdc.cam.ac.uk/conts/retrieving.html.

RESULTS AND DISCUSSION

Synthesis and General Characterization. All five novel cationic trigonal prismatic $[Na_4Ni_{24}Dy_4(BTC4A)_6L_3(CO_3)_6(OH)_8Cl_4(H_2O)_{10}]^{10+}$ HMONCs are obtained through a stepwise approach by utilizing presynthesized $Na_2Ni_{12}Ln_2$ (Ln = Dy and Tb) clusters with linear dicarboxylate ligands. The phase purities of these HMONCs are determined by powder X-ray diffraction (PXRD), which are in agreement with those simulated on the basis of the single-crystal X-ray diffraction data (Figures S14−S18, in the Supporting Information). Moreover, thermogravimetric measurements of all these HMONCs suggest that their frameworks can be maintained at more than 300 °C (Figure S13, in the Supporting Information).

Structure of HMONCs. X-ray analysis reveals that the structure of HMONC-**1** is exactly what we predict. It is crystallized in the hexagonal system with space group *P*63/*m* and is composed of two heterometallic $Na_2Ni_{12}Dy_2$ cluster units bridged by three BDC^{2-} ligands, as shown in Figure 3. The vertex-fused tricubane $Na_2Ni_{12}Dy_2$ cores remain intact in the structure, and three peripheral bridged acetate anions from $Na_2Ni_{12}Dy_2$ clusters are substituted by carboxylate groups from three different BDC^{2-} ligands, while the other three acetate anions coordinated to the Dy^{III} ions of the cluster are replaced by five aqua molecules. Thus, it leads to an unprecedented trigonal prismatic $Na_4Ni_{24}Dy_4$ HMONC, possessing three large quadrilateral windows. The height (the $C_{butyl}\cdots C_{butyl}$ distance) is approximately 3.0 nm, and the windows are almost 9.5 × 6.9 Å^2 for HMONC-**1**, respectively. Upon packing, the discrete nanocages are stacked through weak interactions into a three-dimensional supramolecular structure with inner cavities and external channels along each axis (Figure S3, in the Supporting Information). Moreover, the composition and stability of dissolved HMONC-**1** in solution are confirmed by MS (Figure S6, in the Supporting Information). The major peaks at *m*/*z*

DOI: 10.1021/ic502677g
Inorg. Chem. XXXX, XXX, XXX−XXX

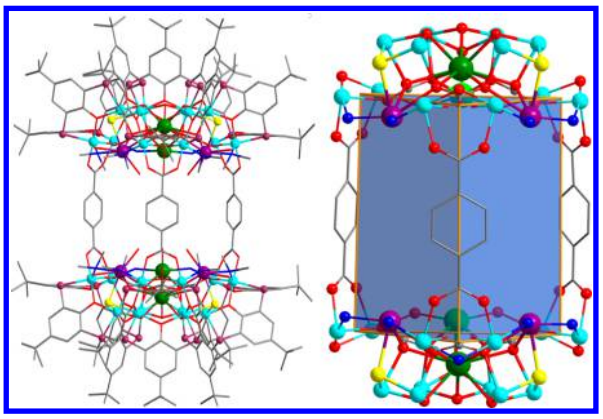

Figure 3. A discrete heterometallic coordination nanocage (left) and the arrangement of vertex-fused tricubane $Na_2Ni_{12}Ln_2$ MBBs and BDC^{2-} ligands (right) in HMONC-**1**. Color code as in Figure 1.

1348.9 and 897.0 can be assigned to $\{[Na_4Ni_{24}Dy_4(BTC4A)_6(BDC)_3(CO_3)_6(Cl)_4(OH)_8(dma)_8(H_2O)_8] + 4H\}^{6+}$ and $\{[Na_4Ni_{24}Dy_4(BTC4A)_6(BDC)_3(CO_3)_6(Cl)_4(OH)_8(H_2O)_8] + H\}^{9+}$ charged species corresponding to the HMONC-**1**, respectively.

Through the above-mentioned stepwise synthetic strategy, we tried to expand the height of HMONC-**1** by replacing H_2BDC ligands with H_2NDC and H_2BPDC, which led to the isolation of HMONC-**2** and HMONC-**3**, respectively. It should be noted that the heights increased to 3.2 and 3.4 nm and the quadrilateral windows increased to 9.5 × 9.1 and 9.5 × 11.2 $Å^2$ for HMONC-**2** and HMONC-**3**, respectively (Figure 4). These

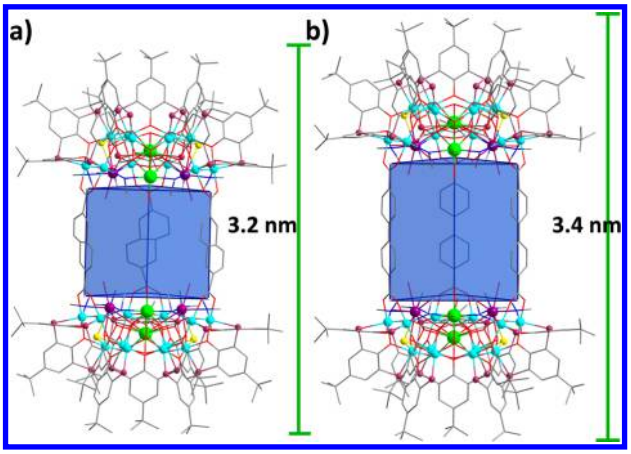

Figure 4. Molecule structures, heights, and windows of HMONC-**2** (a) and HMONC-**3** (b).

quadrilateral windows are larger than the trigonal windows of octahedral TM_{24} MONCs based on TM_4-calix MBBs and BDC^{2-} ligands.[11b,f] Moreover, we also endeavored to introduce the active sites by ligand modification to obtain an analogous structure, which may cause different physicochemical attributes and thus extend their applications such as in environmental or catalytic field.[14] Fortunately, by employing functional organic ligand H_2BIPY as linkers, we have obtained HMONC-**4**. This result highlights the possibility to functionalize our HMONC system. Moreover, the stepwise synthetic method is also proven to be suitable for constructing HMONC-**5** by using compound **1b**, which is isostructural to HMONC-**1**.

Furthermore, if we regard the heterometallic $Na_2Ni_{12}Ln_2$ core as a metal vertex, it is obvious that these trigonal prismatic $Na_4Ni_{24}Ln_4$ HMONCs can seem to be assembled through an M_2L_3 condensation through a stepwise method (M = metal vertex, L = ligand). Although the M_2L_3 condensation has been also found in the construction of other MONCs, they are constructed by mononuclear vertexes.[15] Moreover, the stepwise method has already been utilized in construction of HMONCs, almost all of which are synthesized by employing predesigned metalloligands to react with additional metal ions.[12,16] In contrast, HMONCs using heterometallic clusters as MBBs have not been reported except for a series of cuboid Ir−M (M = Cu, Ni, and Zn) HMONCs via the presynthesized planar heterobimetallic Ir_4M_2 MBBs and different bridging dipyridyl ligands presented by Jin and co-workers.[9] However, the heterotrimetallic $Na_2Ni_{12}Ln_2$ MBBs herein are based on smaller Ni_4-BTC4A MBBs and other linkers, which have not been seen in any other cages. Moreover, all these $Na_4Ni_{24}Ln_4$ HMONCs present the highest nuclearity examples of 3d-4f heterometallic compounds in metal−calixarene systems to date. Overall, this two-step synthetic process sheds some light onto the predictable design and construction of coordination cages or extended networks including predesigned nanocages using presynthesized polymetallic clusters as building subunits.[17]

Magnetic Properties. The HMONCs **1**−**4** built from $Na_2Ni_{12}Dy_2$ cores and linear dicarboxylate ligands are structurally analogous, so we only take the magnetic measurements of HMONC-**1** as an example to investigate whether the heterometallic $Na_2Ni_{12}Dy_2$ core keeps its magnetic properties. The temperature dependence of magnetic susceptibility is performed on the polycrystalline sample of HMONC-**1** in the 2−300 K range under an applied field of 1 kOe, as shown in Figure 5a. At room temperature, the $\chi_m T$ value is 80.78, which is close to the theoretical value of 80.68 cm^3 K mol^{-1} for 4 noninteracting Dy^{III} ions ($^6H_{15/2}$, g = 4/3) and 24 uncoupled Ni^{II} ions (S = 1, g = 2) (Scheme 2, in the Supporting Information). Upon cooling, the $\chi_m T$ value gradually decreases and then falls rapidly to 8.02 cm^3 K mol^{-1} at 2 K. The data of χ_m^{-1} vs T above 50 K obey well the Curie−Weiss equation ($1/\chi_m = T/C - \theta/C$) with the Curie constant C = 81.50 cm^3 mol^{-1} K and Weiss constant θ = −9.62 K. The negative θ value and the gradual decline of $\chi_m T$ values at higher temperatures may be ascribed to the following reasons: the presence of antiferromagnetic interaction (AF) between the metal ions as well as the thermal depopulation of the Stark levels of Dy^{III} ions. The frequency dependent ac susceptibilities under zero dc field were also measured for HMONC-**1** (Figure 5b), from which a frequency dependent out-of-phase signal appears, but the maximum value of χ'' was not observed even at the low temperature (2 K). This phenomenon is likely owing to the fast quantum tunneling of the magnetization. No obvious hysteresis loop was observed for HMONC-**1** (Figure S7, in the Supporting Information). Moreover, the magnetic behaviors of HMONC-**5** were also studied (Figures S8−S10, in the Supporting Information). All the observed magnetic behaviors are similar to the reported heterometallic $Na_2Ni_{12}Ln_2$ cluster (Ln = Dy and Tb).[13] Therefore, it is available to introduce the predictable properties into the resulting structures.

Gas Sorption Properties. To confirm the architectural rigidity and permanent porosity of these HMONCs after activation, the N_2, H_2, and CO_2 adsorption measurements of HMONCs **1**−**4** are determined. All N_2 sorption shows pseudotype I isotherms with saturated N_2 uptake of 238, 257,

DOI: 10.1021/ic502677g
Inorg. Chem. XXXX, XXX, XXX−XXX

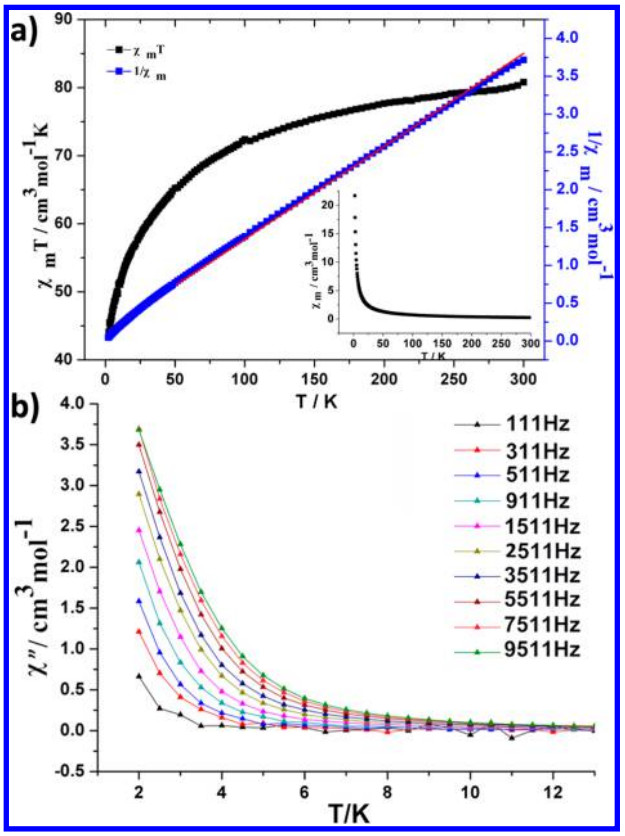

Figure 5. (a) Temperature dependence of magnetic susceptibilities of HMNOC-**1** in a 1000 Oe field. The solid line is the best fit to the Curie–Weiss law. (b) Temperature dependence of the out-of-phase components of the ac magnetic susceptibilities for HMNOC-**1** in a zero dc field and a 3 Oe ac field. Inset: Plot of χ_m vs T for HMNOC-**1** in a 1000 Oe field.

288, and 301 $cm^3\ g^{-1}$ at 77 K and 1.0 bar, revealing that these possesses permanent porosity (Figure 6). The apparent Langmuir and Brunauer–Emmett–Teller surface areas are carried out from the N_2 adsorption data to be 746, 778, 828, and 868 $m^2\ g^{-1}$ and 634, 662, 687, and 704 $m^2\ g^{-1}$ for HMONC-**1**, -**2**, -**3**, and -**4**, respectively. All four HMONCs

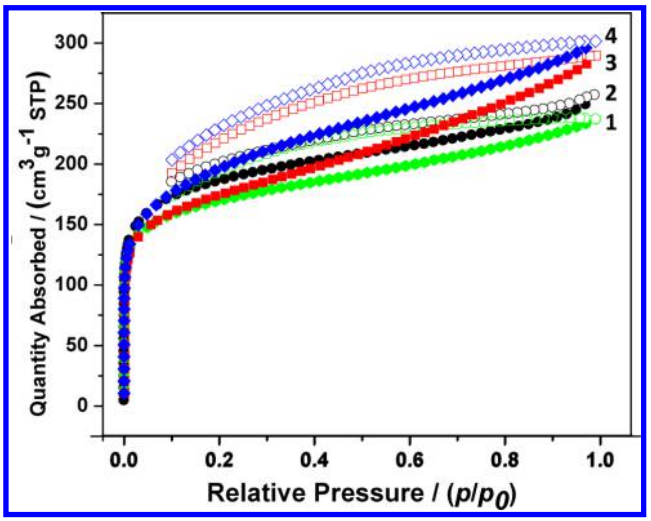

Figure 6. Nitrogen gas sorption isotherms of activated HMONCs. Solid and open circles represent adsorption and desorption data.

show adsorption/desorption hysteresis in N_2 sorption isotherms, which may be ascribed to the structural inhomogeneity or poor uniformity in the crystal size distribution.[8e]

Meanwhile, we also measure volumetric H_2 uptake at 77 and 87 K. The H_2 uptake capacities of these HMONCs are in the range of 76.91–91.78 $cm^3\ g^{-1}$ at 77 K and 1.0 bar, and 59.82–68.32 $cm^3\ g^{-1}$ at 87 K and 1.0 bar (Figure S11, in the Supporting Information), respectively. These values are comparable to the reported thiacalix[4]arene-based coordination cages.[11b,f] Moreover, the isosteric heats of adsorption (Q_{st}) for H_2 are simulated by using the Clausius–Clapeyron equation from the above collected H_2 adsorption data, and their values are estimated to be in the 10.47–11.76 kJ mol^{-1} range at zero coverage (Figure 7), and all four decrease slowly with incessant

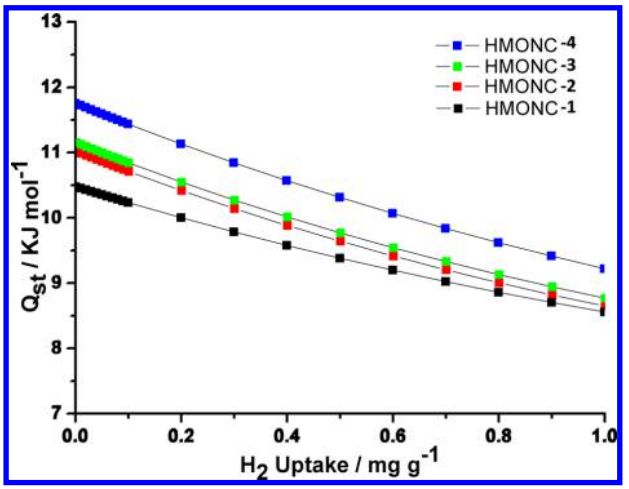

Figure 7. Adsorption heats (Q_{st}) of hydrogen for HMONC-**1**, -**2**, -**3**, and -**4**.

H_2 loading. It should be noted, these Q_{st} values for H_2 are comparable to those of the well-known IRMOP-51, which are based on $Fe_3O(CO_2)_3(SO_4)_3$ MBBs and $BPDC^{2-}$ linkers,[8b] but higher than those for planar graphite (4 kJ/mol) and activated carbons (6.4 kJ/mol). We assume that the high Q_{st} values of these HMONCs might be owing to the slits and/or narrow channels, which may enhance the interaction between H_2 molecules and the HMONCs. Furthermore, they adsorb 35.54–53.36 $m^3\ g^{-1}$ of CO_2 at 273 K and 1 bar (Figure S12, in the Supporting Information).

CONCLUSIONS

In summary, we present the design and syntheses of a series of trigonal prismatic HMONCs with predictable structures by a stepwise method under solvothermal conditions. In the structure of each HMONC, three linear dicarboxylate ligands link together two heterotrimetallic thiacalix[4]arene-based $Na_2Ni_{12}Ln_2$ MBBs to form a novel cationic $Na_4Ni_{24}Ln_4$ HMONC through a M_2L_3 condensation. As we know, these are the first examples of nanocages based on such high-nuclearity heterotrimetallic MBBs. This stepwise synthetic strategy is observed in the trigonal prismatic $Na_4Ni_{24}Ln_4$ HMONCs, which may provide a good example to explore other coordination nanocages or extended aggregates incorporating predesigned cages with functional properties by the judicious choice of presynthesized polynuclear clusters as building blocks and organic ligands as linkers.

DOI: 10.1021/ic502677g
Inorg. Chem. XXXX, XXX, XXX–XXX

■ ASSOCIATED CONTENT

Supporting Information

Crystallographic data in CIF format, additional figures, magnetic data, sorption data, TGA curves, and PXRD patterns for title HMNOCs. This material is available free of charge via the Internet at http://pubs.acs.org.

■ AUTHOR INFORMATION

Corresponding Author

*E-mail: hmc@fjirsm.ac.cn.

Notes

The authors declare no competing financial interest.

■ ACKNOWLEDGMENTS

This work was financially supported by the 973 Program (2011CB932504), National Natural Foundation of China (21390392, 21131006), and Deanship of Scientific Research (DSR), King Abdulaziz University, Jeddah (1-130-1434-HiCi).

■ REFERENCES

(1) (a) Sun, Q. F.; Iwasa, J.; Ogawa, D.; Ishido, Y.; Sato, S.; Ozeki, T.; Sei, Y.; Yamaguchi, K.; Fujita, M. *Science* **2010**, *328*, 1144−1147. (b) Sun, Q. F.; Sato, S.; Fujita, M. *Nat. Chem.* **2012**, *4*, 330−333. (c) Cook, T. R.; Zheng, Y. R.; Stang, P. J. *Chem. Rev.* **2013**, *113*, 734−777. (d) Seidel, S. R.; Stang, P. J. *Acc. Chem. Res.* **2002**, *35*, 972−983.

(2) (a) Liu, T. F.; Chen, Y. P.; Yakovenko, A. A.; Zhou, H. C. *J. Am. Chem. Soc.* **2012**, *134*, 17358−17361. (b) Li, J.-R.; Yakovenko, A. A.; Lu, W.; Timmons, D. J.; Zhuang, W.; Yuan, D.; Zhou, H.-C. *J. Am. Chem. Soc.* **2010**, *132*, 17599−17610.

(3) (a) Fiedler, D.; Leung, D. H.; Bergman, R. G.; Raymond, K. N. *Acc. Chem. Res.* **2005**, *38*, 349−358. (b) Pluth, M. D.; Raymond, K. N. *Chem. Soc. Rev.* **2007**, *36*, 161−171. (c) Kishi, N.; Akita, M.; Yoshizawa, M. *Angew. Chem., Int. Ed.* **2014**, *53*, 3604−3607. (d) Turega, S.; Cullen, W.; Whitehead, M.; Hunter, C. A.; Ward, M. D. *J. Am. Chem. Soc.* **2014**, *136*, 8475−8483.

(4) (a) Jiménez, A.; Bilbeisi, R. A.; Ronson, T. K.; Zarra, S.; Woodhead, C.; Nitschke, J. R. *Angew. Chem., Int. Ed.* **2014**, *53*, 4556−4560. (b) Park, J.; Sun, L.-B.; Chen, Y.-P.; Perry, Z.; Zhou, H.-C. *Angew. Chem., Int. Ed.* **2014**, *53*, 5842−5846. (c) Zhao, D.; Tan, S.; Yuan, D.; Lu, W.; Rezenom, Y. H.; Jiang, H.; Wang, L. Q.; Zhou, H. C. *Adv. Mater.* **2011**, *23*, 90−93.

(5) (a) Pluth, M. D.; Bergman, R. G.; Raymond, K. N. *Acc. Chem. Res.* **2009**, *42*, 1650−1659. (b) Murase, T.; Nishijima, Y.; Fujita, M. *J. Am. Chem. Soc.* **2011**, *134*, 162−164.

(6) (a) Samanta, D.; Mukherjee, P. S. *Chem.—Eur. J.* **2014**, *20*, 5649−5656. (b) Cui, J.; Gropeanu, R. A.; Stevens, D. R.; Rettig, J.; Campo, A. d. *J. Am. Chem. Soc.* **2012**, *134*, 7733−7740.

(7) (a) Klein, C.; Gütz, C.; Bogner, M.; Topić, F.; Rissanen, K.; Lützen, A. *Angew. Chem., Int. Ed.* **2014**, *53*, 3739−3742. (b) Gütz, C.; Hovorka, R.; Klein, C.; Jiang, Q.-Q.; Bannwarth, C.; Engeser, M.; Schmuck, C.; Assenmacher, W.; Mader, W.; Topić, F.; Rissanen, K.; Grimme, S.; Lützen, A. *Angew. Chem., Int. Ed.* **2014**, *53*, 1693−1698. (c) Yoneya, M.; Yamaguchi, T.; Sato, S.; Fujita, M. *J. Am. Chem. Soc.* **2012**, *134*, 14401−14407. (d) Horiuchi, S.; Murase, T.; Fujita, M. *J. Am. Chem. Soc.* **2011**, *133*, 12445−12447.

(8) (a) Liu, T.; Zhang, Y.-J.; Wang, Z.-M.; Gao, S. *J. Am. Chem. Soc.* **2008**, *130*, 10500−10501. (b) Sudik, A. C.; Millward, A. R.; Ockwig, N. W.; Cote, A. P.; Kim, J.; Yaghi, O. M. *J. Am. Chem. Soc.* **2005**, *127*, 7110−7118. (c) Breen, J. M.; Schmitt, W. *Angew. Chem., Int. Ed.* **2008**, *47*, 6904−6908. (d) Zheng, S.-T.; Zhang, J.; Li, X.-X.; Fang, W.-H.; Yang, G.-Y. *J. Am. Chem. Soc.* **2010**, *132*, 15102−15103. (e) Liu, G.; Ju, Z.; Yuan, D.; Hong, M. *Inorg. Chem.* **2013**, *52*, 13815−13817. (f) Zhang, Z.; Wojtas, L.; Zaworotko, M. J. *Chem. Sci.* **2014**, *5*, 927.

(9) Li, H.; Han, Y. F.; Lin, Y. J.; Guo, Z. W.; Jin, G. X. *J. Am. Chem. Soc.* **2014**, *136*, 2982−2985.

(10) (a) Jin, P.; Dalgarno, S. J.; Atwood, J. L. *Coord. Chem. Rev.* **2010**, *254*, 1760−1768. (b) Kumari, H.; Mossine, A. V.; Kline, S. R.; Dennis, C. L.; Fowler, D. A.; Teat, S. J.; Barnes, C. L.; Deakyne, C. A.; Atwood, J. L. *Angew. Chem., Int. Ed.* **2012**, *51*, 1452−1454. (c) Fowler, D. A.; Rathnayake, A. S.; Kennedy, S.; Kumari, H.; Beavers, C. M.; Teat, S. J.; Atwood, J. L. *J. Am. Chem. Soc.* **2013**, *135* (33), 12184−12187. (d) Karotsis, G.; Evangelisti, M.; Dalgarno, S. J.; Brechin, E. K. *Angew. Chem., Int. Ed.* **2009**, *48*, 9928−9931. (e) Homden, D. M.; Redshaw, C. *Chem. Rev.* **2008**, *108* (12), 5086−5130. (f) Bi, Y. F.; Wang, X. T.; Liao, W. P.; Wang, X. F.; Wang, X. W.; Zhang, H. J.; Gao, S. *J. Am. Chem. Soc.* **2009**, *131*, 11650−11651. (g) Kajiwara, T.; Iki, N.; Yamashita, M. *Coord. Chem. Rev.* **2007**, *251*, 1734−1746. (h) Kumar, R.; Lee, Y. O.; Bhalla, V.; Kumar, M.; Kim, J. S. *Chem. Soc. Rev.* **2014**, *43*, 4824−4870. (i) Pasquale, S.; Sattin, S.; Escudero-Adán, E. C.; Martínez-Belmonte, M.; de Mendoza, J. *Nat. Commun.* **2012**, *3*, 785. (j) Bi, Y. F.; Wang, X. T.; Liao, W. P.; Wang, X. F.; Wang, X. W.; Zhang, H. J.; Gao, S. *J. Am. Chem. Soc.* **2009**, *131*, 11650−11651. (k) Kajiwara, T.; Iki, N.; Yamashita, M. *Coord. Chem. Rev.* **2007**, *251*, 1734−1746. (l) Kumar, R.; Lee, Y. O.; Bhalla, V.; Kumar, M.; Kim, J. S. *Chem. Soc. Rev.* **2014**, *43*, 4824−4870.

(11) (a) Dai, F.-R.; Wang, Z. *J. Am. Chem. Soc.* **2012**, *134*, 8002−8005. (b) Dai, F. R.; Sambasivam, U.; Hammerstrom, A. J.; Wang, Z. *J. Am. Chem. Soc.* **2014**, *136*, 7480−7491. (c) Du, S.; Hu, C.; Xiao, J. C.; Tan, H.; Liao, W. *Chem. Commun.* **2012**, *48*, 9177−9179. (d) Liu, M.; Liao, W.; Hu, C.; Du, S.; Zhang, H. *Angew. Chem., Int. Ed.* **2012**, *51*, 1585−1588. (e) Bi, Y.; Wang, S.; Liu, M.; Du, S.; Liao, W. *Chem. Commun.* **2013**, *49*, 6785−6787. (f) Xiong, K.; Jiang, F.; Gai, Y.; Yuan, D.; Chen, L.; Wu, M.; Su, K.; Hong, M. *Chem. Sci.* **2012**, *3*, 2321. (g) Xiong, K.; Jiang, F.; Gai, Y.; He, Z.; Yuan, D.; Chen, L.; Su, K.; Hong, M. *Cryst. Growth Des.* **2012**, *12*, 3335−3341. (h) Xiong, K. C.; Jiang, F. L.; Gai, Y. L.; Yuan, D. Q.; Han, D.; Ma, J.; Zhang, S. Q.; Hong, M. C. *Chem.—Eur. J.* **2012**, *18*, 5536−5540. (i) Su, K.; Jiang, F.; Qian, J.; Gai, Y.; Wu, M.; Bawaked, S. M.; Mokhtar, M.; Al-Thabaiti, S. A.; Hong, M. *Cryst. Growth Des.* **2014**, *14*, 3116−3123. (j) Su, K.; Jiang, F.; Qian, J.; Wu, M.; Gai, Y.; Pan, J.; Yuan, D.; Hong, M. *Inorg. Chem.* **2014**, *53*, 18−20.

(12) (a) Metherell, A. J.; Ward, M. D. *Chem. Commun.* **2014**, *50*, 6330−6332. (b) Li, K.; Zhang, L. Y.; Yan, C.; Wei, S. C.; Pan, M.; Zhang, L.; Su, C. Y. *J. Am. Chem. Soc.* **2014**, *136*, 4456−4459.

(13) Xiong, K.; Wang, X.; Jiang, F.; Gai, Y.; Xu, W.; Su, K.; Li, X.; Yuan, D.; Hong, M. *Chem. Commun.* **2012**, *48*, 7456−7458.

(14) (a) Bloch, E. D.; Britt, D.; Lee, C.; Doonan, C. J.; Uribe-Romo, F. J.; Furukawa, H.; Long, J. R.; Yaghi, O. M. *J. Am. Chem. Soc.* **2010**, *132*, 14382−14384. (b) Eddaoudi, M.; Kim, J.; Rosi, N.; Vodak, D.; Wachter, J.; O'Keeffe, M.; Yaghi, O. M. *Science* **2002**, *295*, 469−472.

(15) (a) Su, C. Y.; Cai, Y. P.; Chen, C. L.; Lissner, F.; Kang, B. S.; Kaim, W. *Angew. Chem., Int. Ed.* **2002**, *41*, 3371−3375. (b) Reger, D. L.; Semeniuc, R. F.; Smith, M. D. *Inorg. Chem.* **2003**, *42*, 8137−8139. (c) Mishra, A.; Dubey, A.; Min, J. W.; Kim, H.; Stang, P. J.; Chi, K. W. *Chem. Commun.* **2014**, *50*, 7542−7544.

(16) (a) Wu, H. B.; Wang, Q. M. *Angew. Chem., Int. Ed.* **2009**, *48*, 7343−7345. (b) Hiraoka, S.; Sakata, Y.; Shionoya, M. *J. Am. Chem. Soc.* **2008**, *130*, 10058−10059. (c) Duriska, M. B.; Neville, S. M.; Moubaraki, B.; Cashion, J. A.; Halder, G. J.; Chapman, K. W.; Balde, C.; Letard, J. F.; Murray, K. S.; Kepert, C. J.; Batten, S. R. *Angew. Chem., Int. Ed.* **2009**, *48*, 2549−2552.

(17) (a) Fowler, D. A.; Mossine, A. V.; Beavers, C. M.; Teat, S. J.; Dalgarno, S. J.; Atwood, J. L. *J. Am. Chem. Soc.* **2011**, *133*, 11069−11071. (b) Tan, H.; Du, S.; Bi, Y.; Liao, W. *Chem. Commun.* **2013**, *49*, 8211−8213.

(18) Lhotak, P.; Smejkal, T.; Stibor, I.; Havlicek, J.; Tkadlecova, M.; Petrickova, H. *Tetrahedron Lett.* **2003**, *44*, 8093−8097.

(19) Sheldrick, G. M., *SHELXS-97, Program for crystal Structure Solution and Program for crystal Structure Refiniement*; University of Göttingen: Göttingen,1997.

(20) van der Sluis, P.; Spek, A. L. *Acta Crystallogr., Sect. A* **1990**, *46*, 194−201.

DOI: 10.1021/ic502677g
Inorg. Chem. XXXX, XXX, XXX−XXX